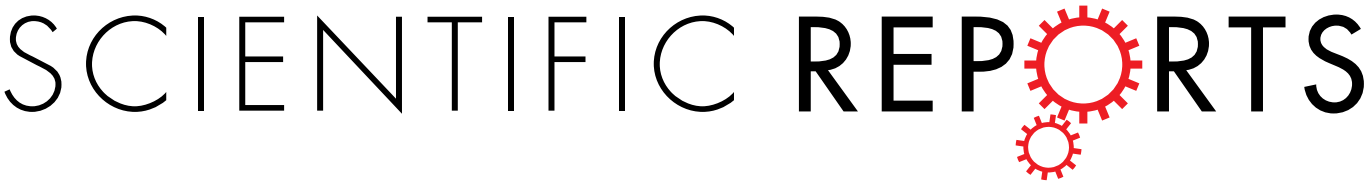

OPEN

Highly efficient Fenton and enzyme-mimetic activities of NH_2-MIL-88B(Fe) metal organic framework for methylene blue degradation

Received: 27 October 2017
Accepted: 15 March 2018
Published online: 26 March 2018

Jianchuan He[1,2], Yao Zhang[1], Xiaodan Zhang[1] & Yuming Huang[1]

Here, we show that NH_2-MIL-88B(Fe) can be used as a peroxidase-like catalyst for Fenton-like degradation of methylene blue (MB) in water. The iron-based NH_2-MIL-88B(Fe) metal organic framework (MOF) was synthesized by a facile and rapid microwave heating method. It was characterized by scanning electron microscopy, Fourier transform infrared spectroscopy, powder X-ray diffraction, and the Brunauer–Emmett–Teller method. The NH_2-MIL-88B(Fe) MOF possesses intrinsic oxidase-like and peroxidase-like activities. The reaction parameters that affect MB degradation were investigated, including the solution pH, NH_2-MIL-88B(Fe) MOF and H_2O_2 concentrations, and temperature. The results show that the NH_2-MIL-88B(Fe) MOF exhibits a wide working pH range (pH 3.0–11.0), temperature tolerance, and good recyclability for MB removal. Under the optimal conditions, complete removal of MB was achieved within 45 min. In addition, removal of MB was above 80% after five cycles, showing the good recyclability of NH_2-MIL-88B(Fe). The NH_2-MIL-88B(Fe) MOF has the features of easy preparation, high efficiency, and good recyclability for MB removal in a wide pH range. Electron spin resonance and fluorescence probe results suggest the involvement of hydroxyl radicals in MB degradation. These findings provide new insight into the application of high-efficient MOF-based Fenton-like catalysts for water purification.

Metal organic frameworks (MOFs) are composed of metal ions with organic linkers. They have received great attention because of their peculiar structural properties, such as large specific surface areas, tuneable porosities, good thermal stabilities, and uniform structured nanoscale cavities. Various MOF structures have been designed and synthesized for a wide variety of applications, including separation, storage of molecules, sensors, luminescence, and catalysis[1–6], among which chemical catalysis is particularly interesting[6–10]. However, investigation of the catalytic applications of MOFs has mainly focused on model organic reactions[7–10]. Recently, several MOFs, including Fe-containing MOFs (MIL-101(Fe), MIL-53(Fe), MIL-88B(Fe), $(Me_3Sn)_4Fe(CN)_6$, and MIL-53(Fe)), have been investigated as photocatalysts for CO_2 reduction[11], Cr(VI) reduction[12], and reactive dye degradation[13–17]. In addition, MIL-100(Fe) and Fe^{II}@MIL-100(Fe) have been used as Fenton-like catalysts for removal of azo-dye from wastewater[18]. However, low pH (pH 3.0) is needed to obtain high catalytic performance, and total organic carbon (TOC) removal by Fe^{II}@MIL-100(Fe) in the first 8 h is low (13–29%)[18]. Zhao *et al.*[19] found that MOF(2Fe/Co)/carbon aerogel shows good electrocatalytic and photocatalytic activities. They showed that it can be used to design a solar photo-electro-Fenton process for removal of rhodamine B and dimethyl phthalate at the optimal pH of 3.0. Li *et al.*[20] reported an Fe(II) bipyridinedicarboxylate based MOF as a Fenton catalyst for degradation of phenol in the narrow pH range of 3–6. Martínez *et al.*[21] reported that Fe-BTC and MIL-100(Fe) can be used as Fenton catalysts for MB removal with TOC reduction of about 55% in 60 min at an initial pH of 4. However, the limited operational pH range and the need for acidic conditions (pH 3.0–4.0) for the degradation

[1]The Key Laboratory of Eco-environments in Three Gorges Reservoir Region, Ministry of Education, College of Chemistry and Chemical Engineering, Southwest University, Chongqing, 400715, PR China. [2]School of Basic Medical Sciences, North Sichuan Medical College, Nanchong, 637000, PR China. Correspondence and requests for materials should be addressed to Y.H. (email: yuminghuang2000@yahoo.com)

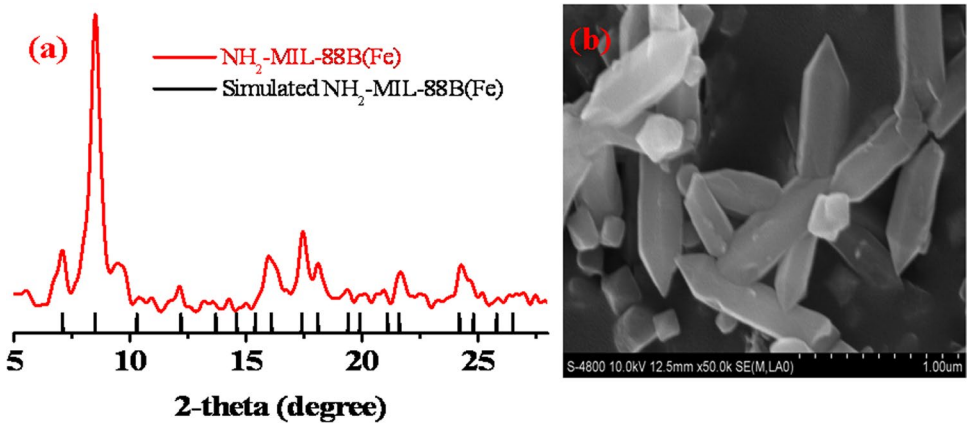

Figure 1. (**a**) The PXRD patterns of the as-prepared NH_2-MIL-88B(Fe) (red line) and the simulated patterns of the NH_2-MIL-88B(Fe) (black short bars). (**b**) SEM image of the as-prepared NH_2-MIL-88B(Fe).

reaction (i.e., the water must be acidified) in the above studies are drawbacks that hinder the use of the MOFs in water purification. Most recently, MOFs have been reported to exhibit peroxidase-like catalytic activity[22–26]. This opens the door for development of MOF-based nanoscale platforms for sensing application in the bioanalytical field[27,28]. However, research of MOFs as enzyme mimetics in an aqueous environment is rare. The first member of enzyme-like active MOFs is PCN-222(Fe) with porphyrinic Fe(III) centers[22]. Subsequently, MIL-53(Fe), MIL-68(Fe), and MIL-100(Fe) with intrinsic peroxidase-like catalytic activity have been developed[23–26]. Application of these active MOFs as peroxidase mimetics for colorimetric biosensing has also been proposed. These studies demonstrate the potential of MOFs as mimic enzymes. However, application of MOF-based mimic enzymes is still limited. There have been no reports of using MOFs as mimic enzymes with wide pH tolerance and good recyclability for degradation of toxic dyes in water by a Fenton-like reaction.

Herein, we report removal of methylene blue (MB) by Fe-based MOFs (i.e., NH_2-MIL-88B(Fe) MOF) to evaluate the potential of using MOFs as peroxidase mimic catalysts in the Fenton-like reaction for removal of organic dyes from contaminated water. The NH_2-MIL-88B(Fe) MOF was synthesized by a fast and facile microwave-assisted approach[29]. Interestingly, the as-prepared NH_2-MIL-88B(Fe) MOF shows intrinsic oxidase-like activity, peroxidase-like activity, and excellent catalytic performance for MB degradation by a Fenton-like reaction in a wide pH range. The narrow pH range remains a limitation for removal of organic pollutants from water using Fenton-based reactions[30,31]. The catalytic mechanism of NH_2-MIL-88B(Fe) was investigated and a possible mechanism is proposed based on electron spin resonance (ESR) and fluorescence probe results for detection of ·OH free radicals, which confirms the major role of ·OH free radicals in degradation of MB. The adsorption isotherm for adsorption of MB on NH_2-MIL-88B(Fe) was determined and the adsorption kinetics was investigated. The effects of NH_2-MIL-88B(Fe) MOF and H_2O_2 concentrations, solution pH, and reaction temperature were also investigated based on the MB and TOC removal efficiencies. Finally, the reusability of NH_2-MIL-88B(Fe) was investigated. The results show the rapid and good recyclability of NH_2-MIL-88B(Fe) for removal of MB from wastewater in a wide pH range by a Fenton-like reaction.

Results and Discussion

Characterization and enzyme-like activity of NH_2-MIL-88B(Fe). NH_2-MIL-88B(Fe) was synthesized by a microwave-assisted approach, which has attracted growing attention as a promising way to synthesize MOF materials[29,32–37]. It has the advantages of speed, high efficiency, and high yield[29,32]. However, the microwave-assisted approach has rarely been applied for synthesis of NH_2-MIL-88B(Fe)[29]. In this work, the NH_2-MIL-88B(Fe) MOF was synthesized by microwave heating with a yield of ca. 30%. The crystal structure of the as-prepared material was confirmed to be NH_2-MIL-88B(Fe) by powder X-ray diffraction (PXRD) (Fig. 1a), which is in agreement with a previous report[29] and indicates the success of NH_2-MIL-88B (Fe) synthesis. It is noted that the PXRD pattern of NH_2-MIL-88B(Fe) in this work is different from that in Shi's work[12]. This could be caused by the difference in the solvents used for treatment of as-prepared NH_2-MIL-88B(Fe)[29]. Similar to previous work, the scanning electron microscopy (SEM) image shows that the synthesized NH_2-MIL-88B(Fe) has a needle-shaped morphology[29] with needle sizes of approximately 800 nm in length and 300 nm in diameter (Fig. 1b). Successful formation of NH_2-MIL-88B(Fe) was further confirmed by Fourier transform infrared (FTIR) spectroscopy (Fig. S1, Supporting Information). The characteristic absorption peaks associated with NH_2-MIL-88B(Fe) are observed at around 3490 and 3370 cm^{-1}, corresponding to the symmetric and asymmetric stretching vibrations of the primary amine groups. The peak at around 1700 cm^{-1} is attributed to the carboxylic group. The FTIR spectrum is the same as those of previous studies[24,37]. The specific surface area of NH_2-MIL-88B(Fe) MOF was calculated to be 163.9 m^2/g.

Before using NH_2-MIL-88B(Fe) in the Fenton-like reaction, the enzyme-like activity of NH_2-MIL-88B(Fe) was evaluated by oxidizing the typical peroxidase substrate 3,3′,5,5′-tetramethylbenzidine (TMB) in the presence and absence of H_2O_2. As shown in Fig. 2a, similar to other enzyme mimic reactions, the typical absorbance peak of the oxidation product of TMB is located at 652 nm[38,39]. The absorbance of the peak at 652 nm significantly increases in the presence of NH_2-MIL-88B(Fe), confirming the peroxidase-like activity of NH_2-MIL-88B(Fe).

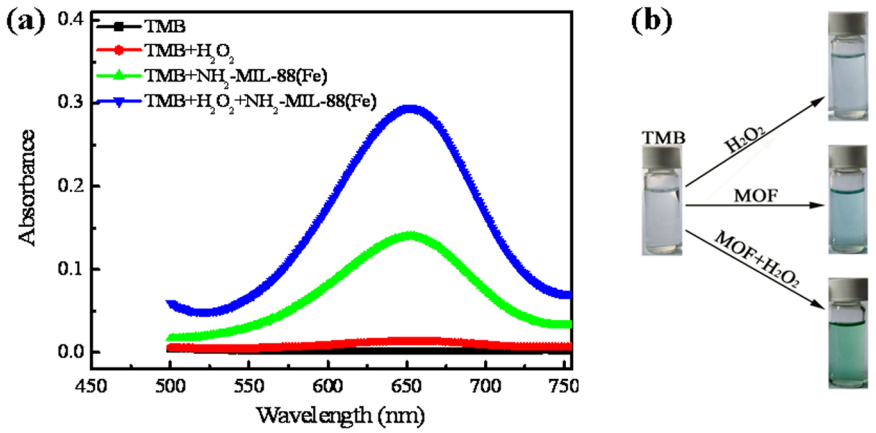

Figure 2. (**a**) UV/vis spectroscopy of 0.05 mM TMB after 20-min reaction with and without 0.1 mM H_2O_2 in 0.2 M acetate buffer (pH 4.0) in the absence and presence of 40 mg/L NH_2-MIL-88B(Fe). (**b**) Images colour reaction of TMB oxidation by H_2O_2 or dissolved O_2 in the absence and presence of NH_2-MIL-88B(Fe).

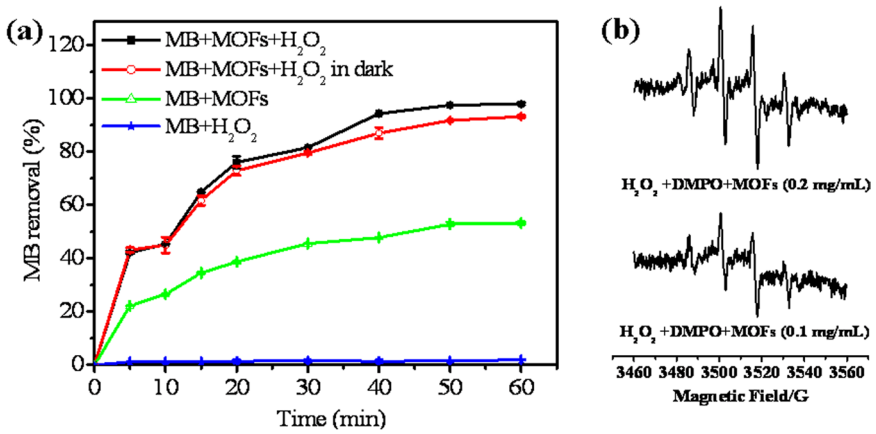

Figure 3. (**a**) MB removal versus time in the absence and presence of H_2O_2 and NH_2-MIL-88B(Fe) on different conditions. Reaction conditions: pH 5.6, 0.2 g/L of NH_2-MIL-88B(Fe), 0.2 M of H_2O_2, 20 mg/L of MB. Error bars represent one standard deviation for three measurements. (**b**) The effect of the concentration of NH_2-MIL-88B(Fe) on the hydroxyl radical formation in the H_2O_2-DMPO system.

Interestingly, even in the absence of H_2O_2, NH_2-MIL-88B(Fe) can catalyze oxidation of TMB by dissolved O_2 to produce the typical colour reaction (Fig. 2b), indicating that NH_2-MIL-88B(Fe) also exhibits oxidase-like activity. Thus, NH_2-MIL-88B(Fe) can potentially be used as an enzyme mimic catalyst in the Fenton-like reaction for removal of organic pollutants in the presence of H_2O_2.

Role of NH_2-MIL-88B(Fe) in Fenton-like removal of MB dye. As-synthesized NH_2-MIL-88B(Fe) was applied as a Fenton-like catalyst for removal of MB as a model organic dye. Figure 3a shows the kinetics of MB removal in the presence and absence of H_2O_2 and NH_2-MIL-88B(Fe). Slight removal of MB occurs in the absence of NH_2-MIL-88B(Fe), indicating that direct oxidation of MB by H_2O_2 is limited. In contrast, when only the NH_2-MIL-88B(Fe) catalyst is present in the MB solution, the removal efficiency increases with increasing reaction time. The peak removal efficiency of about 52% occurs at 50 min, which is mainly caused by adsorption of MB on NH_2-MIL-88B(Fe). Notably, when both NH_2-MIL-88B(Fe) and H_2O_2 are present in the solution of MB, almost 100% removal of MB is achieved after 50 min. The above observation confirms that about half of the MB removal is attributed to NH_2-MIL-88B(Fe) acting as a strong peroxidase mimic in aqueous media. This is probably because degradation of MB by H_2O_2 in the presence of NH_2-MIL-88B(Fe) mainly originates from generation of highly active ·OH free radicals. The presence of ·OH free radicals in the catalytic process was confirmed by ESR spectroscopy. The ESR spectrum in the presence of NH_2-MIL-88B(Fe) shows the four-fold characteristic peak of the typical DMPO–·OH adduct with an intensity ratio of 1:2:2:1 (Fig. 3b), suggesting that NH_2-MIL-88B(Fe) can decompose H_2O_2 to ·OH radicals. Furthermore, the intensity of the characteristic peak increases with increasing NH_2-MIL-88B(Fe) concentration (Fig. 3b), confirming the catalytic ability of NH_2-MIL-88B(Fe) to decompose H_2O_2 to ·OH radicals. MOFs have previously been used as photocatalysts to degrade active dyes[13–17]. Interestingly, as a control, when the mixture of NH_2-MIL-88B(Fe), MB, and H_2O_2 was placed in the dark, there was no significant change in MB removal (Fig. 3a). This suggests that NH_2-MIL-88B(Fe) shows high catalytic activity for MB removal without the need for light irradiation, further confirming the peroxidase-like activity of

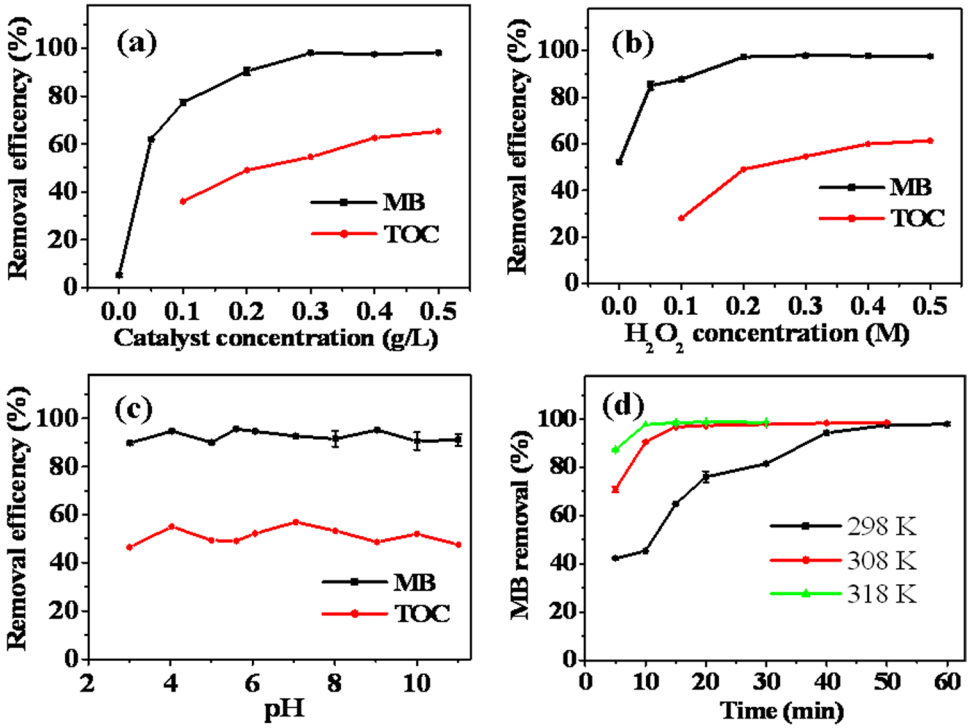

Figure 4. (**a**) Effect of catalyst concentration on the removal of MB and TOC (25 °C, pH 5.6, concentration of H_2O_2: 0.2 M, concentration of initial MB: 20 mg/L). (**b**) Effect of H_2O_2 concentration on the removal of MB and TOC (25 °C, pH 5.6, catalyst concentration: 0.2 g/L, concentration of initial MB: 20 mg/L). (**c**) Effect of solution pH on the removal of MB and TOC (25 °C, catalyst concentration: 0.2 g/L, concentration of H_2O_2: 0.2 M, concentration of initial MB: 20 mg/L). (**d**) Effect of reaction temperature on the removal of MB (pH 5.6, catalyst concentration: 0.2 g/L, concentration of H_2O_2: 0.2 M, concentration of initial MB: 20 mg/L).

NH_2-MIL-88B(Fe). Hence, NH_2-MIL-88B(Fe) can be used as an effective peroxidase mimic catalyst for removal of MB without the need for light irradiation.

Recently, MOFs have been used for removal of hazardous organic compounds, such as benzene[36], dyes[40–45], nitrobenzene[46,47], pharmaceuticals and personal care products[48,49], phenolic compounds[50,51], aniline[51], herbicides[52], and organoarsenic compounds[53], form aqueous media for water purification. This demonstrates that MOFs are promising materials for organic pollution clean-up. In our case, a significant fraction of MB (52%) was removed by direct adsorption to NH_2-MIL-88B(Fe). To understand the adsorption performance, the time-dependent adsorption capacity was determined to investigate the kinetics of adsorption of MB on NH_2-MIL-88B(Fe). The kinetics of MB adsorption on NH_2-MIL-88B(Fe) shows a rapid initial uptake stage and a subsequent stable stage (Fig. S2, Supporting Information), indicating rapid adsorption of MB on NH_2-MIL-88B(Fe). The pseudo-first-order and pseudo-second-order equations were used to fit the adsorption kinetics data (Supporting Information). The correlation coefficient for the pseudo-second-order kinetic model is high (>0.99) (Table S1, Supporting Information). The pseudo-second-order model fits the experimental data better than the pseudo-first-order model (Table S1, Supporting Information). Similar results have been obtained for adsorption of MB on MOF-235[41] and methyl orange on Cr-BDCs, such as MIL-53 and MIL-101[42]. Interestingly, the kinetic constant for MB adsorption on NH_2-MIL-88B(Fe) is larger than that for adsorption of MB on MOF-235[41] (Table S2, Supporting Information), confirming the fast removal rate of MB by NH_2-MIL-88B(Fe).

The adsorption isotherm was determined after adsorption/desorption equilibrium for 1 h (Fig. S2, Supporting Information). The adsorption isotherm of MB on NH_2-MIL-88B(Fe) is shown in Fig. S3 (Supporting Information). The Langmuir and Freundlich models were used to describe adsorption of MB on NH_2-MIL-88B(Fe) (Supporting Information). The results show that the Langmuir model is suitable to describe adsorption of MB on NH_2-MIL-88B(Fe) (Table S3, Supporting Information). The maximum adsorption capacity (Q_{max}) of NH_2-MIL-88B(Fe) for MB is 61.46 mg/g. This can be attributed to electrostatic interaction between the positive charge of MB and the negative charge of COO^-, which is verified by the zeta potential of NH_2-MIL-88B(Fe) (Fig. S4, Supporting Information). The surface charge of NH_2-MIL-88B(Fe) remains negative. Thus, adsorption of positively charged MB on negatively charged NH_2-MIL-88B(Fe) could be by electrostatic attraction. The charge-balancing anion of NH_2-MIL-88B(Fe)[41] and $\pi-\pi$ interaction[54] between the benzene rings of NH_2-MIL-88B(Fe) MOF and MB could also be responsible for MB adsorption.

Optimization of the experimental conditions for Fenton-like degradation of MB. The effect of NH_2-MIL-88B(Fe) concentration on MB degradation was investigated in the range 0–0.5 g/L, and the results are shown in Fig. 4a. The MB degradation efficiency increases from 5% to 90% with increasing NH_2-MIL-88B(Fe)

concentration from 0 to 0.2 g/L. This enhancement in the degradation efficiency is because of an increase in the ·OH radicals (Fig. 3b). As the amount of NH_2-MIL-88B(Fe) increases, more hydroxyl radicals are generated. However, with a further increase in the NH_2-MIL-88B(Fe) concentration, there is only a slight change in the MB removal efficiency. It is interesting to note that TOC removal steadily increases with increasing NH_2-MIL-88B(Fe) concentration from 0.1 to 0.5 g/L, and the maximum TOC removal of 65.1% occurs at a NH_2-MIL-88B(Fe) concentration of 0.5 g/L. Obviously, the removal efficiency of TOC increases as the catalyst concentration increases, while that of MB gets plateau at 0.3 g/L NH_2-MIL-88B(Fe). This is because the color removal or decolorization is ascribed to the destruction of the whole molecular or the chromophore destruction, while TOC removal is attributed to the mineralization of the organic pollutants. Hence, 100% color removal may not mean the completely mineralization of organic pollutants[55]. At a NH_2-MIL-88B(Fe) concentration of 0.3 g/L, the color removal was as high as 97% above, while the TOC removal was only 54.6% (Fig. 4a). Thus, a further increase in catalyst dosage above 0.3 g/L caused no obvious decolorization of MB, although H_2O_2 decomposition was accelerated as the dose of NH_2-MIL-88B(Fe) increased and more hydroxyl radicals generated (Fig. 3b). This suggests that some organic intermediates with low molecules were generated[56] and incompletely mineralization of MB. Hence, TOC removal steadily increases with increasing NH_2-MIL-88B(Fe) concentration. This rapid reduction in the TOC could be related to the enhanced generation of ·OH radicals at a high concentration of NH_2-MIL-88B(Fe). Considering that 90% MB removal efficiency and about 50% mineralization of MB are achieved at 0.2 g/L NH_2-MIL-88B(Fe), 0.2 g/L was chosen as the NH_2-MIL-88B(Fe) concentration in the subsequent experiments.

The effect of H_2O_2 concentration on the degradation efficiency of MB and TOC removal was investigated, and the results are shown in Fig. 4b. The experimental results show that the degradation efficiency of MB rapidly increases with increasing concentration of H_2O_2 in the range 0–0.2 M. However, there is only a slight change in MB removal when the concentration of H_2O_2 is above 0.2 M. TOC removal steadily increases with increasing H_2O_2 concentration in the range 0–0.5 M, and the maximum TOC removal of 61.3% occurs when the H_2O_2 concentration is 0.5 M. In this work, the optimized H_2O_2 concentration was set at 0.2 M.

The solution pH is an important factor that can remarkably affect catalytic reactions. Thus, the effect of pH on the degradation efficiency of MB and TOC removal was investigated in the pH range 3.0–11.0 (Fig. 4c). The pH has no significant influence on degradation of MB, and the MB removal efficiency is in the range 88.1–95.5% for the studied pH range. The results for TOC removal are similar and there is a high level of mineralization of MB (47–57%) in the studied pH range. The results show that NH_2-MIL-88B(Fe) can effectively work in a wide pH range. This is different from the conventional Fenton reaction, which usually requires acidic conditions. This wide pH range can simplify the treatment procedure for practical application and lower the treatment cost. Therefore, the pH of the MB solution was not adjusted for the subsequent experiments.

The effect of temperature on the degradation efficiency of MB and TOC removal was also investigated. The degradation efficiency of MB and TOC removal are plotted against time at different temperatures in Figs 4d and S5 (Supporting Information). The degradation efficiency of MB and TOC removal are higher at higher temperature. Only 15 min is needed for complete removal of MB when the temperature is $\geq$308 K (Fig. 4d). This shows that the NH_2-MIL-88B(Fe) MOF has high temperature tolerance because it can effectively work at a high temperature (318 K), and it is superior to most natural enzymes. The TOC abatement efficiency reaches 41.44% after 30 min reaction at room temperature (Fig. S5, Supporting Information). Hence, for operational convenience and practical consideration, room temperature was chosen for the following experiments.

Possible catalytic mechanism. To determine the catalytic mechanism of NH_2-MIL-88B(Fe), hydroxyl radical formation was investigated using terephthalic acid (TA) as a fluorescence probe. The hydroxyl radical can readily react with TA, forming highly fluorescent 2-hydroxyterephthalic acid[57]. As shown in Fig. S6 (Supporting Information), the fluorescence intensity of TA is weak in the absence of NH_2-MIL-88B(Fe). However, it increases with increasing amount of NH_2-MIL-88B(Fe). This suggests that ·OH is generated by H_2O_2 decomposition. H_2O_2 decomposition accelerates as the amount of NH_2-MIL-88B(Fe) increases and more hydroxyl radicals are generated, which was confirmed by ESR spectroscopy (Fig. 3b). The above observations confirm that the oxidation mechanism of MB catalyzed by NH_2-MIL-88B(Fe) can be ascribed to generation of ·OH by decomposition of H_2O_2. *p*-Benzoquinone (BQ) was also used to investigate the possible active intermediate in the reaction system, because it has been reported that BQ is a good trapper of $O_2^{\bullet-}$ radicals[58]. The results indicate that MB degradation is inhibited in the presence of BQ (Fig. S7, Supporting Information), suggesting that $O_2^{\bullet-}$ radicals are formed in catalytic degradation of MB by H_2O_2 in the presence of NH_2-MIL-88B(Fe). To further confirm this, the effect of superoxide dismutase (SOD, the specific $O_2^{\bullet-}$ scavenger) on the removal of MB was studied. As shown in Table S4, MB removal decreased by more than 28% in the presence of 20 U/mL SOD as the specific $O_2^{\bullet-}$ scavenger, indicating the presence of $O_2^{\bullet-}$ radical in MB removal.

Recycling of NH_2-MIL-88B(Fe). When a MOF is used as a heterogeneous catalyst, its stability under the reaction conditions is an important issue that needs to be considered[10]. Hence, recycling experiments were performed to evaluate the durability of NH_2-MIL-88B(Fe). The results show that MB removal is above 80% after five cycles (Fig. 5). The loss of the catalytic activity is probably related to the nanosize and good dispersibility of NH_2-MIL-88B(Fe) in aqueous solution, leading to its partial recovery by centrifugation. The cumulative loss of Fe ions between the cycles is probably another reason for the observed decline in MB removal, although only a small amount of Fe^{3+} leaches out (<0.5%) at pH 3.0–11.0 and the concentration of dissolved iron in solution is less than 0.2 mg/L (Fig. S8, Supporting Information). In addition, after five cycles, the BET surface area of NH_2-MIL-88B(Fe) decreased from 163.9 m^2/g to 13.5 m^2/g. The obvious decrease in the BET surface area suggests the collapse of NH_2-MIL-88B(Fe) framework, leading to partial loss of crystallinity and cracks of the NH_2-MIL-88B(Fe) (Figs S9 and S10, Supporting Information). This also contributes to the loss of catalytic activities of NH_2-MIL-88B(Fe) after cycles. NH_2-MIL-88B(Fe) can be easily separated from the reaction solution by simple

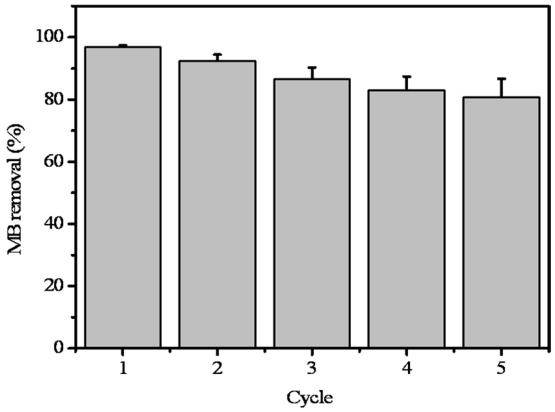

Figure 5. Removal efficiency of MB for different cycles of NH_2-MIL-88B(Fe) using identical reaction conditions. Reaction conditions: pH 5.6, 0.3 g/L of NH_2-MIL-88B(Fe), 0.2 M H_2O_2, 20 mg/L of MB. Error bars represent one standard deviation ($n = 3$).

centrifugation and reused. Thus, no additional chemicals are needed to regenerate NH_2-MIL-88B(Fe), indicating that this MOF is a promising catalyst with potential applications in water purification.

Conclusion

We have successfully synthesized the NH_2-MIL-88B(Fe) MOF by a simple and facile microwave-assisted approach. The as-prepared NH_2-MIL-88B(Fe) exhibits unique oxidase-like and peroxidase-like activities. We used the MOF as a mimic enzyme in the Fenton-like reaction for effective degradation of MB (a model toxic dye) in contaminated water. Complete removal of MB was achieved within 45 min. Regeneration studies show the feasibility of catalyst reuse. Importantly, removal of MB is above 80% after five cycles, showing the high stability of the as-prepared NH_2-MIL-88B(Fe) MOF in aqueous media. Taking into account the easy preparation, wide pH tolerance, high efficiency, and good recycling ability, NH_2-MIL-88B(Fe) is a promising Fenton-like catalyst for water purification.

Experimental Section

Chemicals and reagents. Iron(III) chloride hexahydrate ($FeCl_3 \cdot 6H_2O$), 2-aminoterephthalic acid (NH_2-BDC), TA, ethanol, *N*,*N*-dimethylformamide (DMF), MB, hydrogen peroxide, sodium hydroxide, and hydrochloric acid were purchased from Chongqing Taixin Chemical Co. Ltd. (Chongqing, China). TMB, *p*-benzoquinone, and 5,5-dimethyl-1-pyrroline *N*-oxide (DMPO) were obtained from Sigma-Aldrich (St. Louis, MO, USA) and stored in a refrigerator at 4 °C. All of the analytical reagents were used without further purification. All of the solutions were prepared using ultra-pure water. The solution pH was adjusted using dilute HCl and NaOH solutions.

Preparation of the NH_2-MIL-88B(Fe) MOF. NH_2-MIL-88B(Fe) was prepared by the method reported by Ma *et al.*[29] with slight modification. In brief, $FeCl_3 \cdot 6H_2O$ (124.5 mg, 0.46 mmol), NH_2-BDC (83.4 mg, 0.23 mmol), and DMF (10 mL, 0.13 mol) were mixed by magnetic stirring for 30 min at room temperature to form a solution with a Fe^{3+}/NH_2-BDC/DMF molar ratio of 1:1:282. After the solution was degassed by shaking in an ultrasonic bath for 5 min, the resulting mixture was transferred into a 100 mL Teflon autoclave, which was sealed and placed in a microwave oven (Mars-5, CEM, maximum power 1200 W). The autoclave was heated to 150 °C in about 5 min and then maintained at this temperature for 15 min. The microwave power was set to 600 W throughout the whole synthesis process, including the heating-up stage. After the reaction, the resulting suspension was centrifuged. The obtained solid product was purified by triple treatment in DMF and ethanol at 60 °C for 1 h, and then dried under vacuum at 60 °C overnight. A reddish brown power was obtained with a yield of about 30%.

Instrumentation. The ultraviolet–visible measurements were performed with a UV-2450 Shimadzu spectrophotometer (Suzhou, China). The SEM images were recorded by a Hitachi S-4800 field emission scanning electron microscope (Hitachi, Japan) with an accelerating voltage of 10 kV. The PXRD patterns of the as-prepared products were recorded with a XD-3X-ray diffractometer (PuXi, Beijing, China) under the conditions of nickel-filtered CuKα radiation ($\lambda = 0.15406$ nm) at a current of 20 mA and a voltage of 36 kV. The scanning rate was set to 4°/min. The specific surface area was determined by the Brunauer–Emmett–Teller method using an ASAP 2020 Micromeritics instrument (Maike, USA) at 77 K. The FTIR spectra were recorded with a Nicolet 170SX spectrometer (Madison, WI, USA) in transmission mode using KBr pellets of the sample. The TOC measurements were performed with a Hach IL TOC-550 TOC analyzer (Hach, USA). A MARS-5 microwave heating apparatus was used for preparation of NH_2-MIL-88B(Fe). The ESR spectra were recorded with an X-band Bruker ESP300 E ESR spectrometer (Bruker, Germany).

Catalytic removal experiments. The removal experiments were performed by adding 5 mg of NH_2-MIL-88B(Fe) and H_2O_2 into 25 mL of 20 mg/L MB aqueous solution at room temperature for 45 min reaction time. The resulting mixture was then filtered through a 0.22 μm mixed fibre membrane (Tianjin Automatic Science

Instrument Co., Ltd., Tianjin, China) and used for MB and TOC analysis. To evaluate the stability of the as-prepared NH_2-MIL-88B(Fe) catalyst, after the removal experiment, the resulting mixture was centrifuged and the supernatant was discarded. The isolated NH_2-MIL-88B(Fe) catalyst was directly used for the next cycle. The concentration of MB was determined by measuring the absorbance of the solution at 662 nm. The effect of the free radical inhibitor was evaluated by adding *p*-benzoquinone (an $O_2^{\bullet-}$ radical quencher)[58] into the reaction solution.

References

1. Suh, M. P., Park, H. J., Prasad, T. K. & Lim, D. W. Hydrogen storage in metal-organic frameworks. *Chem, Rev.* **112**, 782–835 (2012).
2. Li, J., Sculley, J. & Zhou, H. C. Metal−organic frameworks for separations. *Chem. Rev.* **112**, 869–932 (2012).
3. Kreno, L. E. *et al*. Metal−organic framework materials as chemical sensors. *Chem. Rev.* **112**, 1105–1125 (2012).
4. Cui, Y., Yue, Y., Qian, G. & Chen, B. Luminescent functional metal−organic frameworks. *Chem. Rev.* **112**, 1126–1162 (2012).
5. Yang, C. X., Ren, H. B. & Yan, X. P. Fluorescent metal-organic framework MIL-53(Al) for highly selective and sensitive detection of Fe^{3+} in aqueous solution. *Anal. Chem.* **85**, 7441–7446 (2013).
6. Dhakshinamoorthy, A. & Garcia, H. Catalysis by metal nanoparticles embedded on metal–organic frameworks. *Chem. Soc. Rev.* **41**, 5262–5284 (2012).
7. Lee, J. *et al*. Metal–organic framework materials as catalysts. *Chem. Soc. Rev.* **38**, 1450–1459 (2009).
8. Corma, A., Garcia, H. & Llabrés i Xamena, F. X. Engineering metal organic frameworks for heterogeneous catalysis. *Chem. Rev.* **110**, 4606–4655 (2010).
9. Dhakshinamoorthy, A., Alvaro, M. & Garcia, H. Commercial metal–organic frameworks as heterogeneous catalysts. *Chem. Commun.* **48**, 11275–11288 (2012).
10. Liu, J. *et al*. Applications of metal–organic frameworks in heterogeneous supramolecular catalysis. *Chem. Soc. Rev.* **43**, 6011–6061 (2014).
11. Wang, D., Huang, R., Liu, W., Sun, D. & Li, Z. Fe-based MOFs for photocatalytic CO_2 reduction: Role of coordination unsaturated sites and dual excitation pathways. *ACS Catal.* **4**, 4254–4260 (2014).
12. Shi, L. *et al*. An amine-functionalized iron(III) metal–organic framework as efficient visible-light photocatalyst for Cr(VI) reduction. *Adv. Sci.* **2**, 1500006 (2015).
13. Ai, L., Zhang, C., Li, L. & Jiang, J. Iron terephthalate metal–organic framework: Revealing the effective activation of hydrogen peroxide for the degradation of organic dye under visible light irradiation. *Appl. Catal. B* **148–149**, 191–200 (2014).
14. Du, J. J. *et al*. New photocatalysts based on MIL-53 metal-organic frameworks for the decolorization of methylene blue dye. *J. Hazard. Mater.* **190**, 945–951 (2011).
15. Etaiw, S. E. H. & El-bendary, M. M. Degradation of methylene blue by catalytic and photo-catalytic processes catalyzed by the organotin-polymer $^3{}_\infty[(Me_3Sn)_4Fe(CN)_6]$. *Appl. Catal. B* **126**, 326–333 (2012).
16. Vu, T. A. *et al*. Isomorphous substitution of Cr by Fe in MIL-101 framework and its application as a novel heterogeneous photo-Fenton catalyst for reactive dye degradation. *RSC Adv.* **4**, 41185–41194 (2014).
17. Xu, W. T. *et al*. Metal–organic frameworks MIL-88A hexagonal microrods as a new photocatalyst for efficient decolorization of methylene blue dye. *Dalton Trans.* **43**, 3792–3798 (2014).
18. Lv, H. *et al*. Efficient degradation of high concentration azo-dye wastewater byheterogeneous Fenton process with iron-based metal-organic framework. *J. Mol. Catal. A* **400**, 81–89 (2015).
19. Zhao, H., Chen, Y., Peng, Q., Wang, Q. & Zhao, G. Catalytic activity of MOF(2Fe/Co)/carbon aerogel for improving H_2O_2 and ·OH generation in solar photo–electro–Fenton process. *Appl. Catal. B* **203**, 127–137 (2017).
20. Li, Y., Liu, H., Li, W., Zhao, F. & Ruan, W. A nanoscale Fe(II) metal–organic framework with a bipyridinedicarboxylate ligand as a high performance heterogeneous Fenton catalyst. *RSC Adv.* **6**, 6756–6760 (2016).
21. Martíneza, F. *et al*. Sustainable Fe-BTC catalyst for efficient removal of mehylene blue by advanced fenton oxidation. *Catal. Today* https://doi.org/10.1016/j.cattod.2017.10.002.
22. Feng, D. *et al*. Zirconium-metalloporphyrin PCN-222: Mesoporous metal–organic frameworks with ultrahigh stability as biomimetic catalysts. *Angew. Chem. Int. Ed.* **51**, 10307–10310 (2012).
23. Ai, L., Li, L., Zhang, C., Fu, J. & Jiang, J. MIL-53(Fe): A metal–organic framework with intrinsic peroxidase-like catalytic activity for colorimetric biosensing. *Chem. Eur. J.* **19**, 15105–15108 (2013).
24. Liu, Y., Zhao, X., Yang, X. & Li, Y. A nanosized metal–organic framework of Fe-MIL-88NH_2 as a novel peroxidase mimic used for colorimetric detection of glucose. *Analyst* **138**, 4526–4531 (2013).
25. Zhang, J. *et al*. Water-stable metal–organic frameworks with intrinsic peroxidase-like catalytic activity as a colorimetric biosensing platform. *Chem. Commun.* **50**, 1092–1094 (2014).
26. Qin, F. *et al*. Hemin@metal–organic framework with peroxidaselike activity and its application to glucose detection. *Catal. Sci. Technol.* **3**, 2761–2768 (2013).
27. Gu, Z. Y., Park, J., Raiff, A., Wei, Z. & Zhou, H. C. Metal–organic frameworks as biomimetic catalysts. *Chem. Cat. Chem.* **6**, 67–75 (2014).
28. Zhao, M., Ou, S. & Wu, C. D. Porous metal–organic frameworks for heterogeneous biomimetic catalysis. *Acc. Chem. Res.* **47**, 1199–1207 (2014).
29. Ma, M. Y. *et al*. Iron-based metal−organic frameworks MIL-88B and NH_2-MIL-88B: High quality microwave synthesis and solvent-induced lattice "breathing". *Cryst. Growth Des.* **13**, 2286–2291 (2013).
30. Liu, H. *et al*. A novel electro-Fenton process for water treatment: reaction-controlled pH adjustment and performance assessment. *Environ. Sc. Technol.* **41**, 2937–2942 (2007).
31. Wang, H. *et al*. Fe_3O_4–MWCNT magnetic nanocomposites as efficient peroxidase mimic catalysts in a Fentonlike reaction for water purification without pH limitation. *RSC Adv.* **4**, 45809–45815 (2014).
32. Haque, E., Khan, N. A., Park, J. H. & Jhung, S. H. Synthesis of a metal–organic framework material, iron terephthalate, by ultrasound, microwave, and conventional electric heating: A kinetic study. *Chem. Eur. J.* **16**, 1046–1052 (2010).
33. Jeff, G. *et al*. Rapid and efficient crystallization of MIL-53(Fe) by ultrasound and microwave irradiation. *Microporous Mesoporous Mater.* **162**, 36–43 (2012).
34. Kang, I. J., Khan, N. A., Haque, E. & Jhung, S. H. Chemical and thermal stability of isotypic metal–organic frameworks: Effect of metal ions. *Chem. Eur. J.* **17**, 6437–6442 (2011).
35. Li, L. *et al*. A synthetic route to ultralight hierarchically micro/mesoporous Al(III)-carboxylate metal-organic aerogels. *Nat. Commun.* **4**, 1774 (2013).
36. Jhung, S. H. *et al*. Microwave synthesis of chromium terephthalate MIL-101 and its benzene sorption ability. *Adv. Mater.* **19**, 121–124 (2007).
37. Pham, M. H., Vuong, G. T., Vu, A. T. & Do, T. O. Novel route to size-controlled Fe-MIL-88B-NH_2 metal-organic framework nanocrystals. *Langmuir* **27**, 15261–15267 (2011).
38. Xie, J. *et al*. Co_3O_4-reduced graphene oxide nanocomposite as an effective peroxidase mimetic and its application in visual biosensing of glucose. *Anal. Chim. Acta* **796**, 92–100 (2013).
39. Liu, S., Lu, F., Xing, R. & Zhu, J. J. Structural effects of Fe_3O_4 nanocrystals on peroxidase-like activity. *Chem. Eur. J.* **17**, 620–625 (2011).

40. Tong, M. *et al*. Influence of framework metal ions on the dye capture behavior of MIL-100 (Fe, Cr) MOF type solids. *J. Mater. Chem. A* **1**, 8534–8537 (2013).
41. Haque, E., Jun, J. & Jhung, S. H. Adsorptive removal of methyl orange and methylene blue from aqueous solution with a metal-organic framework material, iron terephthalate (MOF-235). *J. Hazard. Mater.* **185**, 507–511 (2011).
42. Haque, E. *et al*. Adsorptive removal of methyl orange from aqueous solution with metal-organic frameworks, porous chromium-benzenedicarboxylates. *J. Hazard. Mater.* **181**, 535–542 (2010).
43. Chen, C., Zhang, M., Guan, Q. & Li, W. Kinetic and thermodynamic studies on the adsorption of xylenol orange onto MIL-101(Cr). *Chem. Eng. J.* **183**, 60–67 (2012).
44. Huang, X. X. *et al*. Hierarchically mesostructured MIL-101 metal–organic frameworks: supramolecular template-directed synthesis and accelerated adsorption kinetics for dye removal. *Cryst. Eng. Comm.* **14**, 1613–1617 (2012).
45. Huo, S. H. & Yan, X. P. Metal–organic framework MIL-100(Fe) for the adsorption of malachite green from aqueous solution. *J. Mater. Chem.* **22**, 7449–7455 (2012).
46. Xie, L., Liu, D., Huang, H., Yang, Q. & Zhong, C. Efficient capture of nitrobenzene from waste water using metal–organic frameworks. *Chem. Eng. J.* **246**, 142–149 (2014).
47. Patil, D. V. *et al*. MIL-53(Al): An efficient adsorbent for the removal of nitrobenzene from aqueous solutions. *Ind. Eng. Chem. Res.* **50**, 10516–10524 (2011).
48. Hasan, Z., Jeon, J. & Jhung, S. H. Adsorptive removal of naproxen and clofibric acid from water using metal-organic frameworks. *J. Hazard. Mater.* **209**, 151–157 (2012).
49. Cychosz, K. A. & Matzger, A. J. Water stability of microporous coordination polymers and the adsorption of pharmaceuticals from water. *Langmuir* **26**, 17198–17202 (2010).
50. Maes, M., Schouteden, S., Alaerts, L., Depla, D. & De Vos, D. E. Extracting organic contaminants from water using the metal–organic framework $Cr^{III}(OH)\cdot\{O_2C–C_6H_4–CO_2\}$. *Phys. Chem. Chem. Phys.* **13**, 5587–5589 (2011).
51. Xiao, Y. *et al*. Highly selective adsorption and separation of aniline/phenol from aqueous solutions by microporous MIL-53(Al): A combined experimental and computational study. *Langmuir* **30**, 12229–12235 (2014).
52. Jung, B. K., Hasan, Z. & Jhung, S. H. Adsorptive removal of 2,4-dichlorophenoxyacetic acid (2,4-D) from water with a metal–organic framework. *Chem. Eng. J.* **234**, 99–105 (2013).
53. Jun, J. W. *et al*. Effect of central metal ions of analogous metal–organic frameworks on adsorption of organoarsenic compounds from water: plausible mechanism of adsorption and water purification. *Chem. Eur. J.* **21**, 347–354 (2015).
54. Rocher, V., Siaugue, J. M., Cabuil, V. & Bee, A. Removal of organic dyes by magnetic alginate beads. *Water Res.* **42**, 1290–1298 (2008).
55. Rajoriya, S., Bargole, S., George, S. & Saharan, V. K. Treatment of textile dyeing industry effluent using hydrodynamic cavitation in combination with advanced oxidation reagents. *J. Hazard. Mater.* **344**, 1109–1115 (2018).
56. Wang, Q., Tian, S. & Ning, P. Degradation mechanism of methylene blue in a heterogeneous Fenton-like reaction catalyzed by ferrocene. *Ind. Eng. Chem. Res.* **53**, 643–649 (2014).
57. Ishibashi, K., Fujishima, A., Watanabe, T. & Hashimoto, K. Quantum yields of active oxidative species formed on TiO_2 photocatalyst. *J. Photoch. Photobio. A* **134**, 139–142 (2000).
58. Manring, L. E., Kramer, M. K. & Foote, C. S. Interception of O_2^- by benzoquinone in cyanoaromatic-sensitized photooxygenations. *Tetrahedron Lett.* **25**, 2523–2526 (1984).

Acknowledgements

The financial support by the Natural Science Foundation of China (no. 51678485) and the Fundamental Research Funds for the Central University (XDJK2016D019) are gratefully acknowledged. We also thank Dr. Tim Cooper from Edanz Group (www.edanzediting.com/ac) for English editing a draft of this manuscript.

Author Contributions

J.H. and Y.H. designed experiments and analysis. J.H., Y.Z., and Z.X. carried out the experiments, collected data and carried out data analysis. Y.H. overall supervised the experiment and wrote the main manuscript. All authors discussed results and contributed to the writing and revising the paper.

Additional Information

Supplementary information accompanies this paper at https://doi.org/10.1038/s41598-018-23557-2.

Competing Interests: The authors declare no competing interests.

Publisher's note: Springer Nature remains neutral with regard to jurisdictional claims in published maps and institutional affiliations.